Sponsored by
Office of Equal Opportunity Programs
NASA Headquarters
Washington, DC

NASA
UNIVERSITY RESEARCH CENTERS

TECHNICAL ADVANCES IN AERONAUTICS, SPACE SCIENCES AND TECHNOLOGY, EARTH SYSTEMS SCIENCES, GLOBAL HYDROLOGY, AND EDUCATION

VOLUME II

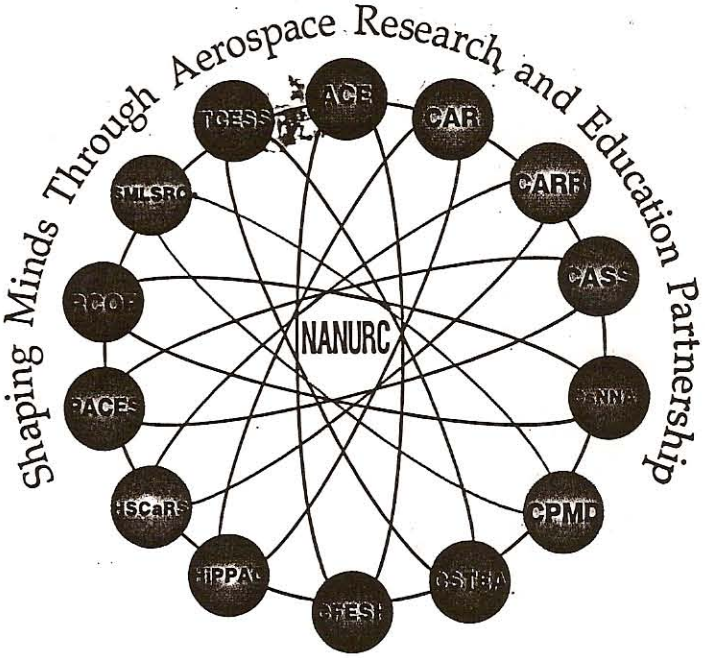

National Alliance of NASA University Research Centers

EDITORS
T. L. Coleman, B. White, and S. Goodman

ASSOCIATE EDITORS
P. Sakimoto, L. Randolph and D. Rickman

Alabama A&M University
Center for Hydrology, Soil Climatology
and Remote Sensing

NASA UNIVERSITY RESEARCH CENTERS SERIES

NASA UNIVERSITY RESEARCH CENTERS TECHNICAL ADVANCES IN AERONAUTICS, SPACE SCIENCES AND TECHNOLOGY, EARTH SYSTEM SCIENCES, GLOBAL HYDROLOGY, AND EDUCATION

VOLUME II

Proceedings of the NASA URC Technical Conference (URC-TC '98)
February 22-25, 1998
Huntsville, Alabama

EDITORS
Tommy L. Coleman
NASA HSCaRS Center, Alabama A&M University

Bettie White
NASA Office of Equal Opportunities, NASA Headquarters

Steven Goodman
NASA Marshall Space Flight Center

ASSOCIATE EDITORS
Philip Sakimoto
NASA Office of Equal Opportunities, NASA Headquarters

Lynwood Randolph
NASA Office of Equal Opportunities, NASA Headquarters

Doug Rickman
NASA Marshall Space Flight Center

'erences

Scientific Assessment of Ozone Depletion: 1994, World Meteorological Organization lobal Ozone Research and Monitoring Project-Report No. 37, 2.16-2.20, (1994).

Mission to Planet Earth (MTPE) Strategic Enterprise Plan 1996-2002, NASA, (1996).

Climate Change, The IPCC (Intergovernmental Panel on Climate Change) Scientific ssessment, Cambridge University Press: New York, Port Chester, Melbourne, Sydney, 990).

Dennis K. Killinger, and Norman Menyuk, "Laser remote sensing of the atmosphere", cience, 235, 37-45 (1987).

. M. Measures, Laser Remote Sensing, Malabar: Krieger Publishing Company, (1992).

N. Nielsen, J. Van der Laan, E. Uthe, W. Bosenberg, R. Kaiser, and C. Carlisle, Development and testing of a compact airbone 3-μm wavelength DIAL", Applied Optics, ıbmitted.

M. J. T. Milton, T. D. Gardiner, G. Chourdakis, and P. T. Woods, "Injection seeding of an ıfrared optical parametric oscillator with a tunable diode laser", Optics Letters, 19, 281-83, (1994).

M. J. T. Milton, R. H. Bradsell, B. W. Jolliffe, N. R. W. Swann, and P. T. Woods, "The esign and development of a near-infrared DIAL system for the detection of hydrocarbons", roceedings of the 14th International Laser Radar Conference, 370-373, (1988).

H. L. Walmsly and S. J. O'Connor, "The measurement of atmospheric emissions from rocess units using differential absorption lidar", in Lidar Atmospheric Monitoring, Jean-ierre Wolf, Editor, Proceedings of SPIC Vol.3104, 60-72, (1997).

W. B. Grant, "Lidar for atmospheric and hydrospheric studies", Tunable Laser Applications edited by F. J. Duarte, New York: Marcel Dekker, (1995), pp 213-305.

J. C. Scoot, R. A. M. Maddever, and A. T. Paton, "Spectroscopy of methane using a Nd:YAG laser at 1.34 μm", Appl. Opt., 31, 815-821, (1992).

W. R. Bosenberg and D. R. Guyer, "Broadly tunable, single-frequency optical parametric frequency-conversion system", J. Opt. Soc. Am. B, 10, 1716-1722, (1993).

T. D. Raymond, P. Esherick, and A. V. Smith, "Widely tunable single-longitudinal-mode pulsed dye laser", Optics Letters, 14, 1116-1118, (1989).

W. R. Bosenberg, L. K. Cheng, and J. D. Bierlein, "Optical parametric frequency conversion properties of KTA," Appl. Phys. Lett., 65, 2765 (1994).

W. Koechner, Solid-state laser engineering, New York: Springer-Verlag, (1992).

B. J. Orr, M. J. Johnson, and J. G. Haub, "Spectroscopic applications of pulsed tunable optical parametric oscillator", Tunable laser applications edited by F. J. Duarte, New York: Marcel Dekker, (1994), pp 11-82.

Fourier Transform Infrared (FT-IR) Spectroscopy of Atmospheric Trace Gases HCl, NO and SO_2

C. Haridass, A. Aw-Musse, E. Dowdye, C. Bandyopadhyay and P. Misra*
Center for the Study of Terrestrial and Extraterrestrial Atmospheres and
Department of Physics and Astronomy
Howard University, Washington, D.C. 20059, U.S.A.

and

H. Okabe
Center for the Study of Terrestrial and Extraterrestrial Atmospheres and
Department of Chemistry
Howard University, Washington, D.C. 20059, U.S.A.

ABSTRACT

Fourier Transform Infrared (FT-IR) spectral data have been recorded in the spectral region 400-4000 cm^{-1} of hydrogen chloride and sulfur dioxide with 1 cm^{-1} resolution and of nitric oxide with 0.25 cm^{-1} resolution, under quasi-static conditions, when the sample gas was passed through tubings of aluminum, copper, stainless steel and teflon. The absorbances were measured for the rotational lines of the fundamental bands of $^1H^{35}Cl$ and $^1H^{37}Cl$ for pressures in the range 100-1000 Torr and for the $^{14}N^{16}O$ molecule in the range 100-300 Torr. The absorbances were also measured for individual rotational lines corresponding to the three modes of vibrations (υ_1-symmetric stretch, υ_2-symmetric bend, υ_3-anti-symmetric stretch) of the SO_2 molecule in the pressure range 25-150 Torr. A graph of absorbance versus pressure was plotted for the observed rotational transitions of the three atmospherically significant molecules, and it was found that the absorbance was linearly proportional to the pressure range chosen, thereby validating Beer's law. The absorption cross-sections were determined from the graphical slopes for each rotational transition recorded for the HCl, NO and SO_2 species. Qualitative and quantitative spectral changes in the FT-IR data will be discussed to identify and characterize various tubing materials with respect to their absorption features.

Key Words: FT-IR, atmospheric, spectroscopy, infrared radiation, absorbance, absorption cross-sections.

INTRODUCTION

At the present time, environmental issues like global climatic change, photochemical smog formation, acid rain, stratospheric ozone hole and deforestation are of great concern worldwide. These issues are related to increasing concentrations of atmospheric trace constituents, such as carbon dioxide (CO_2), nitric oxide and nitrogen dioxide (NO_x), nitrous oxide (N_2O), sulfur dioxide (SO_2), methane (CH_4), and hydrogen chloride (HCl), and their average residence times in the atmosphere.[1] As an illustration, the influence of CO_2, NO_x and N_2O on stratospheric ozone depletion depends on the altitude, and furthermore, CH_4 acts in general against ozone depletion, yet accelerates the depletion within the ozone hole. Measures for reduction of the emissions are either already in effect, or will be implemented, since the concentrations of most of the trace gases, except presumably NO_x and SO_2, are expected to increase further, mainly because of their longevity in the atmosphere. The green house effect[2,3] is related to the radiation budget of the earth and responsible for the fact that the mean earth temperature is 33 °C above its radiation temperature as viewed from space. The contribution of a given gaseous compound to the greenhouse effect is determined by its atmospheric abundance and IR absorptivity. Gases like CO_2 and CH_4 are found to be responsible for more than 80% of the enhancement of the greenhouse effect.[4] Nitric oxide can hinder ozone destruction, which is manifested by low nitric oxide concentration in the ozone hole.

Small concentrations of atmospheric pollutants can also have dramatic effects leading to smog formation. The production of smog is generally restricted to densely populated and industrial areas, where increased concentrations of toxic compounds, such as sulfur dioxide (SO_2), occur near their sources. This type of smog, known as *winter smog* or *London smog*, has lost much of its previous importance owing to drastic reductions in emission of so-called primary pollutants, like sulfur compounds from heating systems. Recently, another type of smog known as *summer smog* or *Los Angeles smog*, has attracted a great deal of interest. This type of smog is produced photochemically from primary pollutants, essentially from NO_x and voltatlic organic compounds (VOCs), under the influence of solar ultraviolet radiation. Hydrochloric acid (HCl), one of many key atmospheric species, is also considered a possible entity in stratospheric ozone depletion. The HCl molecule is formed in the stratosphere predominately by reactions between hydrogen containing species (such as HO_2 and H_2) with CH_4 and Cl radicals. The transport of HCl down into the troposphere, and the competition between various stratospheric photochemical reactions, govern the regeneration of free chlorine and hence its return into the O_3 destruction cycle. This latter process effectively removes Cl from the ClO_x cycle.

Different measurement techniques can be applied to measure the small absorptions encountered in trace detection. Fourier Transform (FT) spectrometers are operated with conventional broad band sources, in conjunction with interferometers, to achieve the desired spectral resolution. FT systems possess higher optical and greater observation time efficiencies, since all spectral elements are simultaneously observed and measured. FT-IR spectrometers are very useful for chemical analyses of multi component mixtures,[5,6] because of the available broad infrared range and simultaneous observations in several spectral regions.

Matrix isolation, in combination with the FT-IR technique [7] has been considered very attractive for laboratory analyses of the composition of sampled air, because it avoids the problem of interferences due to reduction in spectral congestion compared to gas phase spectra. This technique can be applied to a wide range of stable and moderately labile atmospheric trace gases with detection limits in the parts per trillion range. Long-path absorption spectroscopy with lead salt diode lasers has profited from the recent development of tunable IR lasers.[8,9] Very high spectral resolution, together with increased sensitivity and time response, are possible using the technique of tunable diode laser absorption spectroscopy (TDLAS). TDLAS has been performed both with open atmospheric paths and with confined air samples in long-path cells. The technique is not as universal as FT-IR spectroscopy, owing to the limited tuning range of a single diode laser.[10] Fried *et al.*[11] have reported results based on a laboratory study for detecting the important atmospheric molecule HCl using a tunable diode laser coupled with a multipass White cell. These authors also claim that in working with very low concentrations of the highly polar HCl molecule they have encountered problems arising from surface interactions of HCl with the White cell and the inlet plumbing. This has led us to undertake a systematic study of the interaction of atmospheric trace gases like HCl, NO, and SO_2, with the tubing materials used for transporting the gases from the main reservoir to the absorption cell. Thus, in the present work, we report absorption cross-sections of the individual rotational lines of the atmospherically significant molecules, namely HCl, NO, and SO_2, in the gas phase, when these gases were passed through tubes made of different materials, such as aluminum, copper, stainless-steel, and teflon. The measurements were done using a Nicolet Magna-IR 550 Fourier Transform infrared spectrometer. The objective of the present paper was to identify and characterize various tubing materials with respect to their absorption features, so that specific tube-gas combinations may be used to overcome the difficulty of measurement problems associated with a significant loss of sample concentration via adsorption on surfaces of tubings and associated instrumentation.

EXPERIMENTAL

The infrared spectra were recorded using a Nicolet Magna-IR 550 Fourier Transform spectrometer. A 10-m path length multipass absorption cell was used for recording the spectra.[12] A quasi-static system was used for recording the spectra of the sample gases. Tubes of one meter length and made of different materials, namely aluminum, copper, stainless-steel and teflon, were used for recording signature spectra of specific gas samples and to examine the reactivity of the sample with the tubing material. Resolution was set at 1 cm^{-1} for recording of the FT-IR spectra under quasi-static conditions for HCl and SO_2 gases, and at 0.25 cm^{-1} for recording the FT-IR spectra of NO. Thirty six scans (with 1 cm^{-1} and 0.25 cm^{-1} resolution) were co-added after subtraction of the background, each time a sample was examined, and the results were superimposed and averaged for final spectral display. The time required to record each spectrum was less than five minutes. KBr windows were used in the sample cell for better transmission in the mid-infrared region.

Hydrogen chloride (HCl) at a pre-mixed concentration of 529.0 ppm in N_2; nitric oxide (NO) at a pre-mixed concentration of 503.0 ppm in N_2; and sulfur dioxide (SO_2) at a pre-mixed concentration of 484.0 ppm in air, obtained from Scott Speciality Gases, Inc., Plumsteadville, PA ,were used. The absorbances were measured for the rotational lines of the fundamental bands of HCl for pressures in the range 100-1000 Torr, and for the NO molecule in the range 100 - 300 Torr. Absorbances were also measured for the individual rotational lines corresponding to the three modes of vibration (υ_1-symmetric stretch, υ_2-symmetric bend, and υ_3-antisymmetric stretch) of the SO_2 molecule for pressures in the range 25-150 Torr. Characteristic features were obtained for HCl in the spectral range 3100 - 2600 cm^{-1}, for NO in the range 1950 - 1780 cm^{-1}, and for sulfur dioxide in the range 1425 - 400 cm^{-1}. A graph of absorbance versus pressure was plotted for all of the observed rotational lines for the three atmospherically significant molecules, and it was found that the absorbance was linearly proportional to the pressure range chosen, thereby validating the Beer-Lambert law:

$$I = I_0 \exp(-\sigma_v N * l), \qquad (1)$$

where σ_v is the absorption cross section, l the length of the absorption cell and N the molecular density as a function of pressure given by $N = (N_A \times P_{Torr})/RT$, where N_A is the Avogadro Number, P_{Torr} the total pressure of the gas, R the molar gas constant and T the temperature. The absorbance of each line was then given by $A = (I_0/I)$, where I_0 is the incident intensity and I the absorbed intensity.

RESULTS AND DISCUSSION

Hydrogen Chloride: FT-IR Spectra and Analysis

The FT-IR spectra of the fundamental (1-0) band of the diatomic molecule $^1H^{35}Cl$ and its natural abundance isotopomer $^1H^{37}Cl$ were recorded in the spectral range 3100 - 2600 cm^{-1} in dry N_2, at a resolution of 1 cm^{-1}, and with gas pressures of 100-1000 Torr under quasi-static conditions using 1 meter tubes made of aluminum, copper, stainless-steel and teflon, respectively. The main purpose of recording the fundamental band of HCl using the FT-IR spectrometer was to monitor the changes in the intensities of the individual rotational lines in the spectra when the experimental gas was subjected to flow through different tubing materials. The absorbances of ten rotational lines of the P and R branches for both $^1H^{35}Cl$ and $^1H^{37}Cl$ for six different pressures (100, 200, 300, 500, 700 and 1000 Torr) were measured when the gas was flown in turn through aluminum, copper, stainless-steel and teflon tubes. Small changes in the spectra of the experimental gas can be quantitatively understood by calculating the absorption cross-sections for each observed rotational frequency. In the present work, we have calculated the absorption cross-sections by plotting the absorbance versus pressure and using the Beer-Lambert Eqn. (1). . It was found that the absorbance showed a linear relationship to the amount of HCl present in the gas cell, confirming the validity of Beer's Law for the pressure range employed in the experiments (See Fig. 1). Based on the slope of the plot of absorbance versus P_{Torr}, the absorption cross-sections for the observed rotational lines for both $^1H^{35}Cl$ and $^1H^{37}Cl$ were determined. The calculated absorption cross-sections for $^1H^{37}Cl$ are given in Table 1. From the data given in this table, it is evident that there was greater detectable variation in the absorption cross-sections when the gas was passed through aluminum and copper tubings, in contrast to the values of absorption cross-sections obtained when the gas was passed through stainless steel and teflon tubings. The absorption cross-sections for both $^1H^{35}Cl$ and $^1H^{37}Cl$ are shown for comparison in Fig. 2 when the gas was passed through aluminum tubing.

Nitric Oxide: FT-IR Spectra and Analysis

Nitric oxide is produced in the earth's atmosphere mainly by the oxidation of nitrous oxide (N_2O, a by-product of microbial metabolism) by the excited atom of oxygen (in the ^1D state), and to some extent by high-altitude aircraft, nuclear blasts, volcanoes, and lightning.[13] Unlike HCl, the ground state of the NO molecule is a $^2\Pi_r$ state. The rotational structure of a band of the $^2\Pi$-$^2\Pi$ system gives rise to 12 branches. In the present work, because of low resolution (0.25 cm^{-1}), it was possible to observe only the P and R branches of both the $^2\Pi_{1/2}$-$^2\Pi_{1/2}$ and $^2\Pi_{3/2}$-$^2\Pi_{3/2}$ systems as shown in Fig. 3. In the present work, our main goal was to record the fundamental (1-0) band of the nitric oxide molecule using the Fourier Transform spectrometer when the gas was subjected to flow through different tubes made of materials like aluminum, copper, stainless steel and teflon, in order to understand qualitatively and quantitatively the changes in the spectra. Our quantitative analysis was focused mainly on estimating the absorption cross-sections from the observed absorbances at five different pressures (100, 150, 200, 250 and 300 Torr). As mentioned in the previous section, the absorbances of 21 lines of the P and R branches of the two systems were measured for five different pressures. It was found that there was an increase in the absorbance as the pressure of the NO gas was increased in the

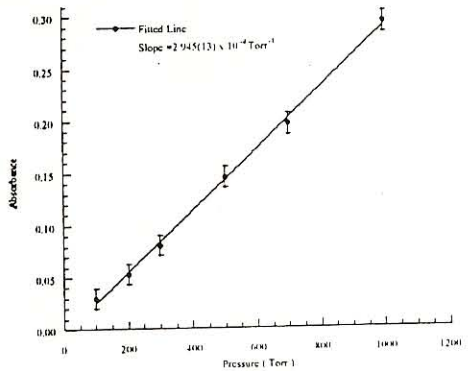

Fig.1. A plot of absorbance versus pressure for the rotational line P(4) of $^1H^{37}Cl$ when the gas was passed through 1 meter teflon tubing.

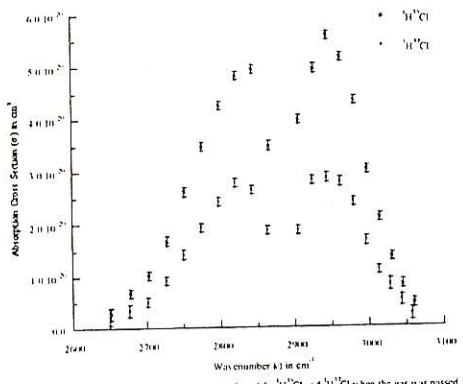

Fig.2. Absorption cross section (σ) versus wavenumber (ν) for $^1H^{35}Cl$ and $^1H^{37}Cl$ when the gas was passed through aluminum tubing.

Table 1. Absorption cross-sections[a] for $^1H^{37}Cl$ (under quasi-static conditions) when the gas was passed through different tubing materials.

	ν (cm^{-1})	Absorption Cross-Section (σ_ν)×10^{20} cm^2				ν (cm^{-1})	Absorption Cross-Section (σ_ν)×10^{20} cm^2			
J	R(J)	Al	Cu	SS	Tef	P(J)	Al	Cu	SS	Tef
0	2904.09	1.87(8)	1.83(8)	1.69(8)	1.67(8)					
1	2923.69	2.83(8)	2.73(8)	2.55(8)	2.53(8)	2862.97	1.87(8)	1.82(8)	1.69(8)	1.68(8)
2	2942.71	2.87(8)	2.78(8)	2.60(8)	2.58(8)	2841.58	2.65(8)	2.55(8)	2.38(8)	2.65(8)
3	2961.10	2.79(8)	2.81(8)	2.55(8)	2.50(8)	2819.51	2.78(8)	2.68(8)	2.50(8)	2.78(8)
4	2978.66	2.40(8)	2.47(8)	2.19(8)	2.13(8)	2796.91	2.43(8)	2.34(8)	2.20(8)	2.43(8)
5	2995.78	1.66(8)	1.60(8)	1.49(8)	1.46(8)	2773.77	1.93(8)	1.87(9)	1.74(8)	1.93(8)
6	3012.12	1.10(8)	1.05(8)	0.98(8)	0.96(8)	2750.09	1.42(8)	1.35(8)	1.27(8)	1.42(8)
7	3027.73	0.8 (1)	0.72(8)	0.66(8)	0.63(8)	2725.88	0.92(8)	0.88(8)	0.84(8)	0.92(8)
8	3042.71	0.5 (1)	0.42(8)	0.38(8)	0.37(8)	2701.13	0.51(8)	0.49(8)	0.45(8)	0.51(8)
9	3056.81	0.3 (1)	0.24(9)	0.19(9)	0.17(8)	2675.96	0.3 (1)	0.29(9)	0.25(9)	0.26(9)
10	3072.92		0.3 (9)	0.2 (8)	0.4 (8)	2650.19	0.2 (2)			0.12(9)

[a]The number in parentheses indicates the estimated error for the absorption cross-section based on the uncertainty in the slope. Abbreviations are: Al-Aluminum: Cu-Copper: SS- Stainless-Steel: Tef: Teflon.

10-m path length cell. Absorption cross-sections were calculated from the slope of the straight line obtained from the absorbance versus pressure plots. The straight line plot confirmed that Beer's law holds good for the pressure range of the NO gas used. Absorption cross-sections were calculated for all the observed rotational lines of both the $^2\Pi_{1/2}$-$^2\Pi_{1/2}$ and $^2\Pi_{3/2}$-$^2\Pi_{3/2}$ systems . Table 2 summarizes the absorption cross-sections for the R and P branches of the $^2\Pi_{1/2}$-$^2\Pi_{1/2}$ transition when the gas was passed through the four tubing materials. A detectable variation in the absorption cross-sections was observed from this table when the gas was passed through aluminum and teflon tubings, as compared to copper and stainless steel tubings.

Sulfur Dioxide: FT-IR Spectra and Analysis

Sulfur dioxide is known as an important constituent for both planetology and astrophysics since it is present on Venus and in interstellar clouds. It is also significant for terrestrial atmospheres because large amounts of SO_2 can be expelled from strong volcanic eruptions. For example, the volcanic eruption of Mount Pinatubo in the Philippines released approximately 20 million tons of sulfur in the atmosphere in June 1991. Once the SO_2 molecules are present in the stratosphere, they are converted into sulfate aerosols, which affect both climate and stratospheric chemistry. Spectroscopic methods are used as standard techniques to track atmospheric concentrations of the SO_2 molecule. High levels of sulfur dioxide were observed from remote infrared measurements shortly after massive volcanic eruptions.[14,15] In the present work, our main goal was to quantitatively determine the reaction of SO_2 with different materials, so that one can emphasize the use of a particular material to transfer the experimental gas from the main reservoir to the absorption cell, and to overcome the loss of concentration from the gaseous adsorption on available surfaces. The fundamental bands of SO_2: ν_1= 1151.71352 cm-1, ν_2=517.8724 cm^{-1} and ν_3=1362.0603 cm^{-1} were recorded using the FT-IR spectrometer at 1 cm^{-1} resolution for five different pressures (25, 50, 75, 100, 125, and 150 Torr) when the gas was passed through aluminum, copper, stainless-steel and teflon tubes. The absorption cross sections were

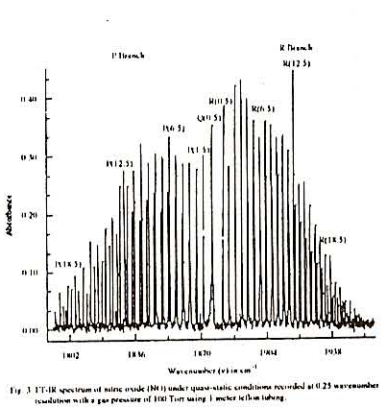

Fig. 3. FT-IR spectrum of nitric oxide (NO) under quasi-static conditions recorded at 0.25 wavenumber resolution with a gas pressure of 100 Torr using 1 meter teflon tubing.

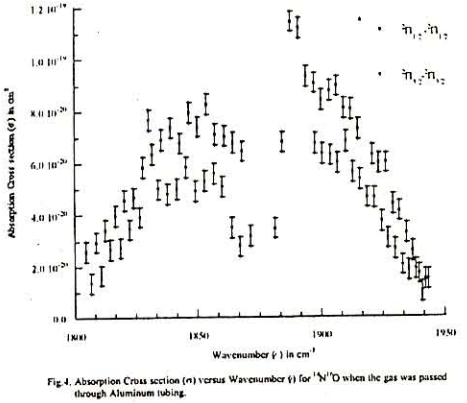

Fig.4. Absorption Cross section (σ) versus Wavenumber (ν) for $^{15}N^{16}O$ when the gas was passed through Aluminum tubing.

Table 2. Absorption cross-sections[a] for the R and P branches of the $^2\Pi_{1/2}$ - $^2\Pi_{1/2}$ transition of $^{14}N^{16}O$ (under quasi-static conditions) when the gas was passed through different tubing materials

	ν (cm^{-1})	Absorption Cross-Section (σ_ν)×10^{20} cm^2				ν (cm^{-1})	Absorption Cross-Section (σ_ν)×10^{20} cm^2			
J	R(J)	Al	Cu	SS	Tef	P(J)	Al	Cu	SS	Tef
0.5	1881.07	3.47(39)	2.92(39)	2.67(39)	3.29(39)					
1.5	1884.34	6.82(39)	5.18(39)	5.48(39)	5.40(39)	1871.08	3.71(39)	2.98(39)	2.77(39)	3.09(55)
2.5	1887.60	11.46(39)	8.29(39)	8.44(39)	8.71(39)	1867.73	6.46(39)	5.73(39)	4.89(39)	5.63(39)
3.5	1890.81	11.22(39)	9.20(39)	8.86(39)	9.36(39)	1864.25	6.79(39)	5.56(39)	4.96(39)	5.95(39)
4.5	1893.94	9.34(39)	7.71(39)	7.62(39)	8.61(39)	1860.79	7.05(39)	5.88(39)	5.98(39)	6.17(39)
5.5	1897.04	9.08(39)	6.92(39)	7.00(39)	7.40(39)	1857.29	7.13(39)	6.23(39)	5.43(39)	6.17(39)
6.5	1900.10	8.44(39)	6.93(39)	6.46(39)	7.18(39)	1853.76	8.26(39)	6.72(39)	6.48(39)	6.60(39)
7.5	1903.16	8.78(39)	6.90(39)	6.67(39)	7.30(39)	1850.19	7.41(39)	6.23(39)	5.90(39)	6.65(39)
8.5	1906.18	8.97(39)	6.89(39)	6.62(39)	7.21(39)	1846.60	7.95(39)	6.23(39)	5.94(39)	6.36(39)
9.5	1909.16	8.10(39)	6.37(39)	6.08(39)	7.02(39)	1842.96	6.78(39)	5.68(39)	5.62(39)	6.24(39)
10.5	1912.10	8.08(39)	6.61(39)	6.09(32)	6.84(39)	1839.30	7.37(39)	6.46(39)	5.64(39)	6.58(39)
11.5	1915.01	7.32(62)	6.05(62)	5.77(39)	6.30(62)	1835.59	6.93(62)	4.84(62)	5.35(39)	5.62(62)
12.5	1917.95	25.38(39)	8.30(39)	7.13(39)	9.51(39)	1831.85	6.35(39)	5.06(39)	5.11(39)	5.15(39)
13.5	1920.74	6.33(39)	4.76(39)	4.75(39)	5.04(39)	1828.08	5.83(39)	4.20(39)	4.61(39)	4.97(39)
14.5	1923.53	6.02(39)	5.09(39)	4.16(39)	5.11(39)	1824.27	4.68(39)	4.20(39)	4.13(39)	4.10(39)
15.5	1926.32	6.02(39)	4.18(39)	3.79(39)	4.34(39)	1820.44	4.56(39)	3.42(39)	3.12(39)	3.54(39)
16.5	1929.06	4.40(39)	3.87(39)	3.55(39)	3.67(39)	1816.56	3.97(39)	3.32(39)	3.03(39)	3.17(39)
17.5	1931.75	4.15(39)	2.92(39)	2.93(39)	3.14(39)	1812.66	3.42(39)	3.10(39)		3.05(39)
18.5	1934.42	3.30(39)	2.48(39)	2.58(39)	2.45(39)	1808.72	2.96(39)	2.08(39)		2.28(39)
19.5	1937.05	2.57(39)	2.02(39)	1.99(39)	2.93(39)	1804.75	2.60(39)	1.88(39)		
20.5	1939.64	1.70(39)	1.70(39)			1800.74		1.77(39)		
21.5	1942.23	1.48(39)	1.48(39)							

[a]same Footnote as in Table 1.

calculated from the slopes of the plots of absorbance versus pressure and are given in Table 5 for the three modes of vibration. An evaluation of the data presented in Table 3 indicates that there was no appreciable variation in the absorption cross-section when the gas was passed through four different materials confirming that the SO_2 gas is fairly inert compared to HCl and NO, as far as reactivity with aluminum, copper, stainless-steel and teflon are concerned.

CONCLUSION

Hydrogen chloride, nitric oxide and sulfur dioxide are trace gases that are present in the atmosphere and are important for the understanding of stratospheric ozone depletion, global warming and smog formation. A sensitive Fourier Transform infrared spectrometer was used to measure the absorbance of HCl, NO and SO_2 for various pressures when the gases were passed separately through four different 1-m long tubings of aluminum, copper, stainless-steel and

ıble 3. Absorption cross-sections[a] for the rotational transition associated with the ν_1, ν_2, and ν_3 vibrational modes of O_2 (under quasi-static conditions) when the gas was passed through different tubing materials

	ν (cm^{-1})	Absorption Cross-Section (σ_ν)×10^{20} cm^2			
No	ν_1 mode	Al	Cu	SS	Tef
1	1122.279	1.71(7)		1.673(3)	1.79(8)
2	1139.683	2.66(7)	2.66(7)	2.62(7)	2.78(9)
3	1163.307	2.97(7)	3.33(7)	3.35(7)	3.48(9)
4	1173.346	2.34(7)	2.25(7)	2.30(7)	2.46(9)

	ν (cm^{-1})	Absorption Cross-Section (σ_ν)×10^{20} cm^2			
No	ν_2 mode	Al	Cu	SS	Tef
1	494.301	2.7(9)	2.56(1)	3.183(7)	3.021(8)
2	497.148	3.15(7)	3.5 (1)	3.10(7)	3.94(7)
3	503.209	4.01(7)	3.77(6)	3.46(7)	4.37(9)
4	522.773	1.87(9)	1.9 (1)	1.54(9)	2.34(9)

No	ν_3 mode	Al	Cu	SS	Tef
1	1342.679	2.14(7)	2.07(7)	2.11(7)	2.18(9)
2	1349.671	2.35(7)	2.28(7)	2.28(7)	2.40(9)
3	1356.880	2.10(7)	2.05(7)	2.04(7)	2.14(9)
4	1371.690	3.04(7)	2.95(7)	2.96(7)	3.14(9)

ame Footnote as in Table 1.

eflon. The absorption cross-sections were determined from the plots of absorbance versus pressure for the observed tational lines of the fundamental bands of HCl, NO and SO_2. The plots confirmed the validity of Beer's law for the ressure range used. Detectable differences in absorbance and absorption cross-sections for the various tubing-gas ombinations were observed. For the HCl molecule, based on the values of the absorption cross-sections, it was oncluded that metallic materials (i.e Al and Cu) showed a greater change in absorption, whereas stainless steel and eflon tubings were comparatively inert. The absorption-cross sections calculated for the NO molecule showed that ere was a greater change in absorption when the gas was passed through aluminum and teflon tubings, as compared o copper and stainless steel tubings. On the other hand, the absorption cross-sections calculated for the SO_2 molecule howed no appreciable variation in absorption when the gas was passed through aluminum, copper, stainless steel and eflon tubings. Thus, we can conclude that great care should be taken in reporting the absolute concentrations of trace olecules of relevance for atmospheric and stratospheric modeling considerations, since one must include the reaction f the gases with tubing materials employed in the inlet and outlet plumbing of the equipment used.

REFERENCES

. Graedel, T. E. and Crutzen, P. J. 1989. The changing atmosphere. *Sci. Am.* 261/9, 28-36.

. Bolin, B., Döös, B. R., Jager, J., and Warrick, R. A., Eds. 1986. *The Greenhouse Effect, climatic Change, and Ecosystems*. Wiley, Chichester.

. Schneider, S. H. 1989. The Changing Climate. *Sci. Am.* 261/9, 38-47.

. Dickinson, R. E. and Cicerone, R. J. 1986. Future global warming from atmospheric trace gases. *Nature (London)*, 319, 109-115.

. Griffiths, P. R. 1975. Chemical Infrared Fourier Transform Spectroscopy, *Chem. Anal.*, 43, Wiley, New York.

. Theophanides, T., Ed. 1984. *Fourier Transform Infrared Spectroscopy*, Reidel, Dordrecht, The Netherlands.

. Almond, M. J. and Downs, A. J. 1989. Spectroscopy of matrix isolated species. *Adv. Spectrosc.* 17.

. Kuritsyn, Yu. A. 1985. Infrared absorption spectroscopy with tunable diode lasers. In *Laser Analytical Spectrochemistry* (V.S. Letokhov, Ed.), Chapter 4. Adam Hilger, Bristol.

. Gristar, R., Böttner, H., Tacke, M., and Restelli, G., Eds. 1992. *Monitoring of Gaseous Pollutants by Tunable Diode Lasers*. Kluwer Academic, Drodrecht, The Netherlands.

0. Schiff, H. 1992. Ground based measurements of atmospheric gases by spectroscopic methods. *Ber. Bunsenges. Phys. Chem.* 96, 296-306.

1. Fried. A., Sams, R., and Berg, W.W. 1984. Application of tunable diode laser absorption for trace stratospheric measurements of HCl: Laboratory results. *Applied Optics*, 23/11, 1867-1880.

2. Aw-Musse, A. 1997. Fourier Transform Infrared (FT-IR) Spectroscopy of Trace Gases HCl And NO of Relevance to Atmospheric Phenomena. M.S. Thesis, Howard University, Washington, D.C.

3. McDermid, I.S. and Landenslager, J. B. 1982. *J. Quant. Spectrosc. Radiat. Transfer*, 27, 483.

4. Mankin, W. G., Coffey, M. T., and Goldman, A. 1992. *Geophys. Res. Lett.*, 19, 179-182.

5. Goodman, J., Snetsinger, K. G., Pueschel, R. F., Ferry, G. V., and Verma, S., 1994. *Geophys. Res. Lett.*, 21, 1129-1132.

ACKNOWLEDGMENTS

The authors would like to acknowledge the financial support received from the *Center for the Study of Terrestrial and Extraterrestrial Atmospheres* (CSTEA) (grant # NAGW-2950), NASA Lewis Research Center (grant # NAG3-1677) and U.S. Environmental Protection Agency's Office of Exploratory Research (grant # R819720-01-3).

Stimulated Raman amplification, oscillation, and linewidth in barium nitrat

Christophe L. McCray and Thomas H. Chyba
Research Center for Optical Physics
Department of Physics
Hampton University
Hampton, Va. 23668
(757) 727-5922 Phone
(757) 727-5955 Fax
cmccray@gprc.hamptonu.edu

Abstract

Measurements of Raman gain in a $Ba(N0_3)_2$ crystal are reported at 532 nm using a Raman oscillator/amplifi arrangement for differential absorption lidar measurements of ozone. The experimentally determined gai coefficient will be compared with theoretical results. The effect of single and multi-longitudinal mode pumpin upon the amplification process will be discussed. Measurement of the Raman linewidth for 1st, 2nd and 3rd stok shifts are presented.

Introduction

The Raman shifting method has been used to help widen the spectral coverage of lase for various applications. Raman shifting is based on stimulated Raman scattering. This is a inelastic scattering process in which light from a laser at wavelength λ_1 is converted into light another wavelength λ_2, which is the result of excitation or deexcitation of an internal resonanc mode in the Raman medium. Radiation at the shifted wavelength λ_2 experiences gain at th expense of the incident laser radiation. Raman scattering occurs in liquids, gases, solids an plasmas. It can involve transitions between electronic states, rotational or molecular vibration lattice vibrations, spin states in semiconductors or electron waves in plasmas. Raman scatterin is a two photon process and obeys the selection rules for two successive dipole transitions [1].

The first single pass Raman scattering in crystalline barium nitrate, $Ba(NO_3)_2$, pumped 1064 nm by a Q-switched frequency doubled, Nd:glass laser was reported in 1980 [2]. Lat work was published on Raman scattering in $Ba(NO_3)_2$ pumped at 532 nm by a Q-switche frequency-doubled, Nd:YAG laser [3,4]. Preliminary experiments [5] at NASA LaRC suggeste that a $Ba(NO_3)_2$ Raman laser could serve as a compact solid state replacement to other existin lasers for uv lidar measurements. A $Ba(NO_3)_2$ Raman crystal pumped at 532 nm by a frequenc doubled Nd:YAG laser will create first Stokes (shifted wavelength) laser output at 563 nm an second Stokes output at 599 nm with very high efficiencies.

Preliminary results on a compact visible $Ba(NO_3)_2$ Raman laser have been obtaine From these initial experiments we obtained a total conversion efficiency greater than 65% at 3 Hz PRF for first and second Stokes [6]. Optimization of the $Ba(NO_3)_2$ laser system can b accomplished by modifying the laser design to better mode match the pump beam with th resonator mode, enabling the pump photons to make more passes in the resonator before leavin the resonator, selecting the mirror reflectivities to suppress unwanted Stokes lines, and b accounting for the thermal lensing and birefringence effects in $Ba(NO_3)_2$.